Study of Limitations to EoR Detection

Nithyanandan Thyagarajan
N. Udaya Shankar
Ravi Subrahmanyan
&
MWA Collaboration

(Raman Research Institute)

Conclusions

- EoR HI power spectrum detections seems feasible with current instruments such as MWA under specific assumptions
- Sample variance and thermal noise are the limiting factors on different scales
- Need for optimal observing strategies & array configuration

HI Power Spectrum

- Statistical detections seem feasible
- Forms a key science of SKA precursors & pathfinders
  - MWA
  - LOFAR
  - GMRT
  - LWA
  - PAPER

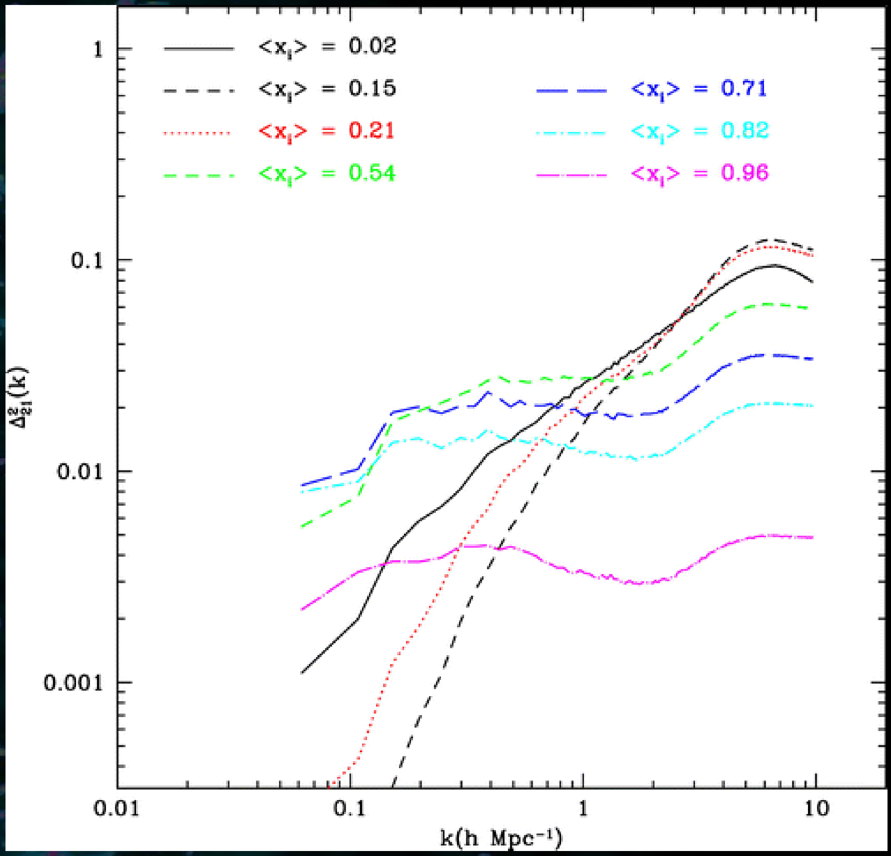

Lidz et al. (2008)

HI EoR Power Spectrum detection seem feasible

Challenges due to Contamination

- Foreground Galactic emission
- Foreground extragalactic radio continuum sources
- Residual Errors after Modeling
- Thermal Noise

Expected sources of contamination

Foreground Removal

- Knowledge of spectral information
  - Galactic modeling
  - Extragalactic source spectral index
- Knowledge of power spectrum symmetry
  - HI power spectrum isotropic
  - Foregrounds not isotropic and contain structure in Fourier space

Morales & Hewitt (2004)

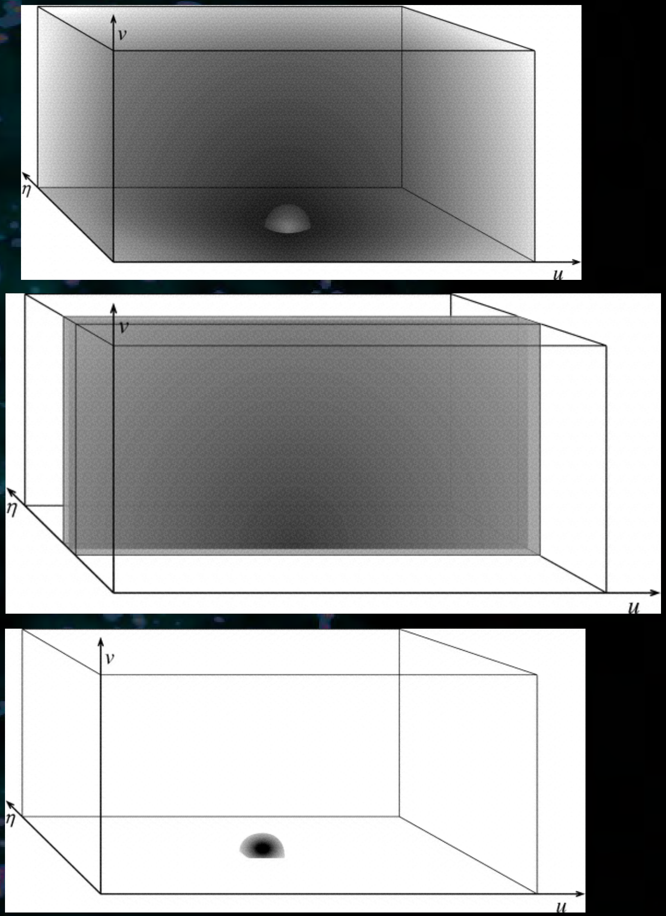

Separation of contamination using symmetries in Fourier space

Contamination after Foreground Removal

- Confusion from unresolved unsubtracted/mis-subtracted sources due to poor angular resolution & limited flux sensitivity (Classical Source Confusion)
- Confusion from sidelobes of frequency dependent beams due to mode-mixing
- Thermal Noise
- Contamination from imaging algorithms (Vedantham et al. 2011)

Our focus on Classical Source Confusion, mode-mixing contamination & Thermal Noise

Framework of our Study

- Radio Source Distribution

$$\mathrm{Log}\left[(\mathrm{d}n/\mathrm{d}S)/(S^{-2.5})\right] = \sum_{i=0}^{6} a_i \left[\mathrm{Log}(S/\mathrm{mJy})\right]^i,$$

- 128-tile MWA Layout

- Relations

$$\{k_x, k_y, k_\parallel\} = 2\pi \left\{ \frac{u}{D_\mathrm{M}(z)}, \frac{v}{D_\mathrm{M}(z)}, \frac{H_0 f_{21} E(z)}{c(1+z)^2}\eta \right\}.$$

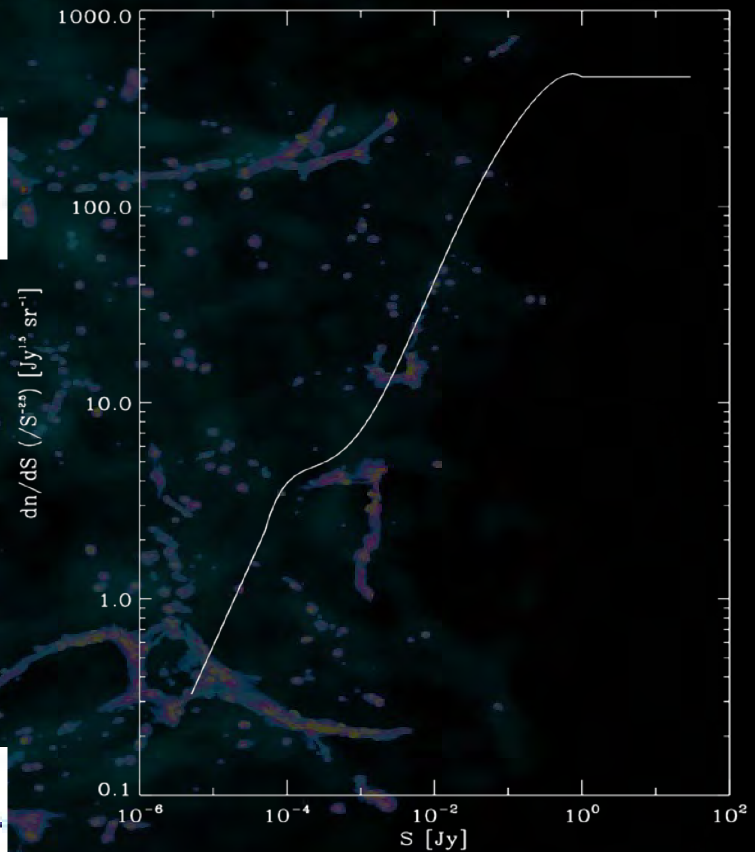

Hopkins et al. (2003)

Classical Confusion in k-space

- Consider zenith pixel
- Smooth variation along frequency of residuals
- Delta function at $k_{||} = 0$
- Array configuration determines variation along k
- Bandpass spillover into EoR window

Bandpass Windows

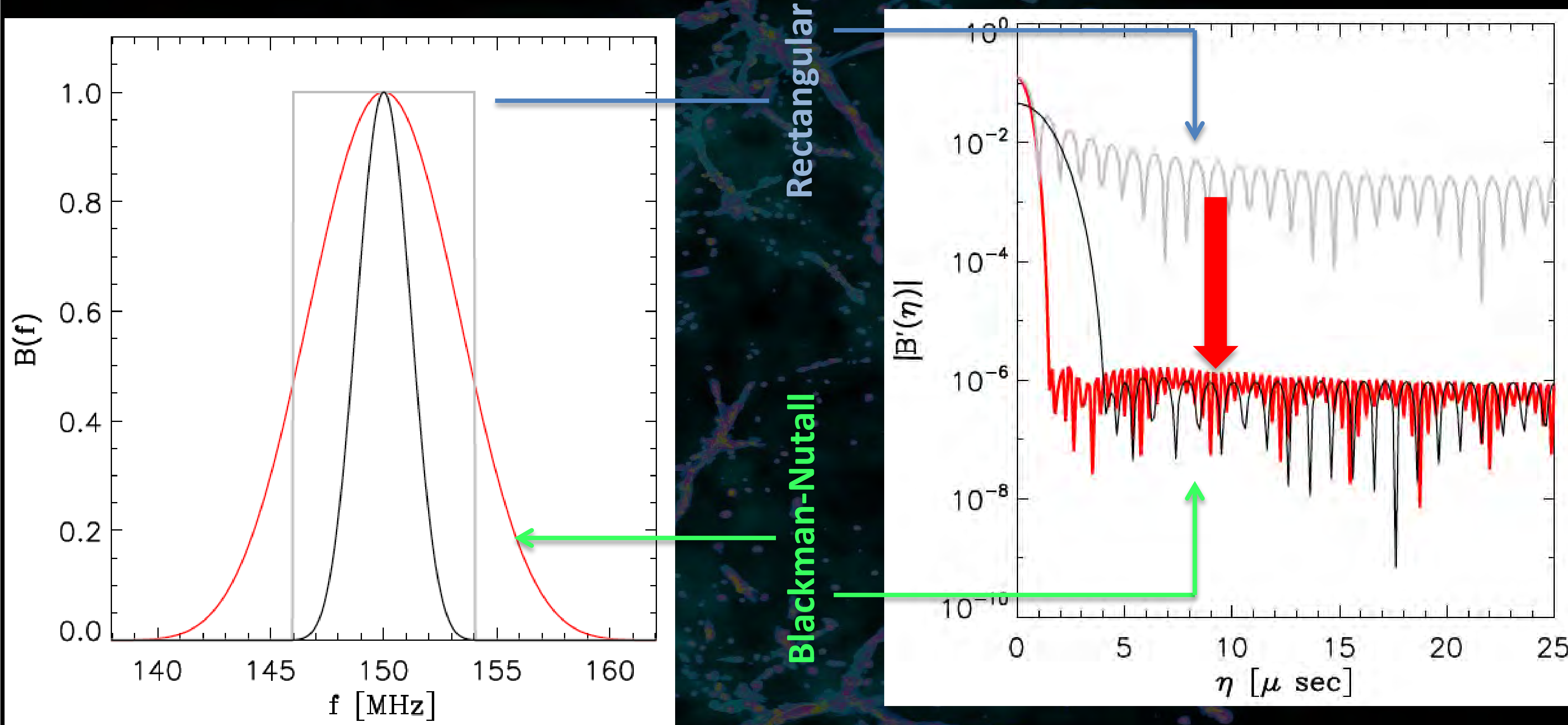

$$B(n) = a_0 - a_1 \cos\left(\frac{2\pi n}{N-1}\right) + a_2 \cos\left(\frac{4\pi n}{N-1}\right) - a_3 \cos\left(\frac{6\pi n}{N-1}\right)$$

Blackman-Nutall window reduces sidelobes by more than 3 orders of magnitude

Classical Confusion in *k*-space

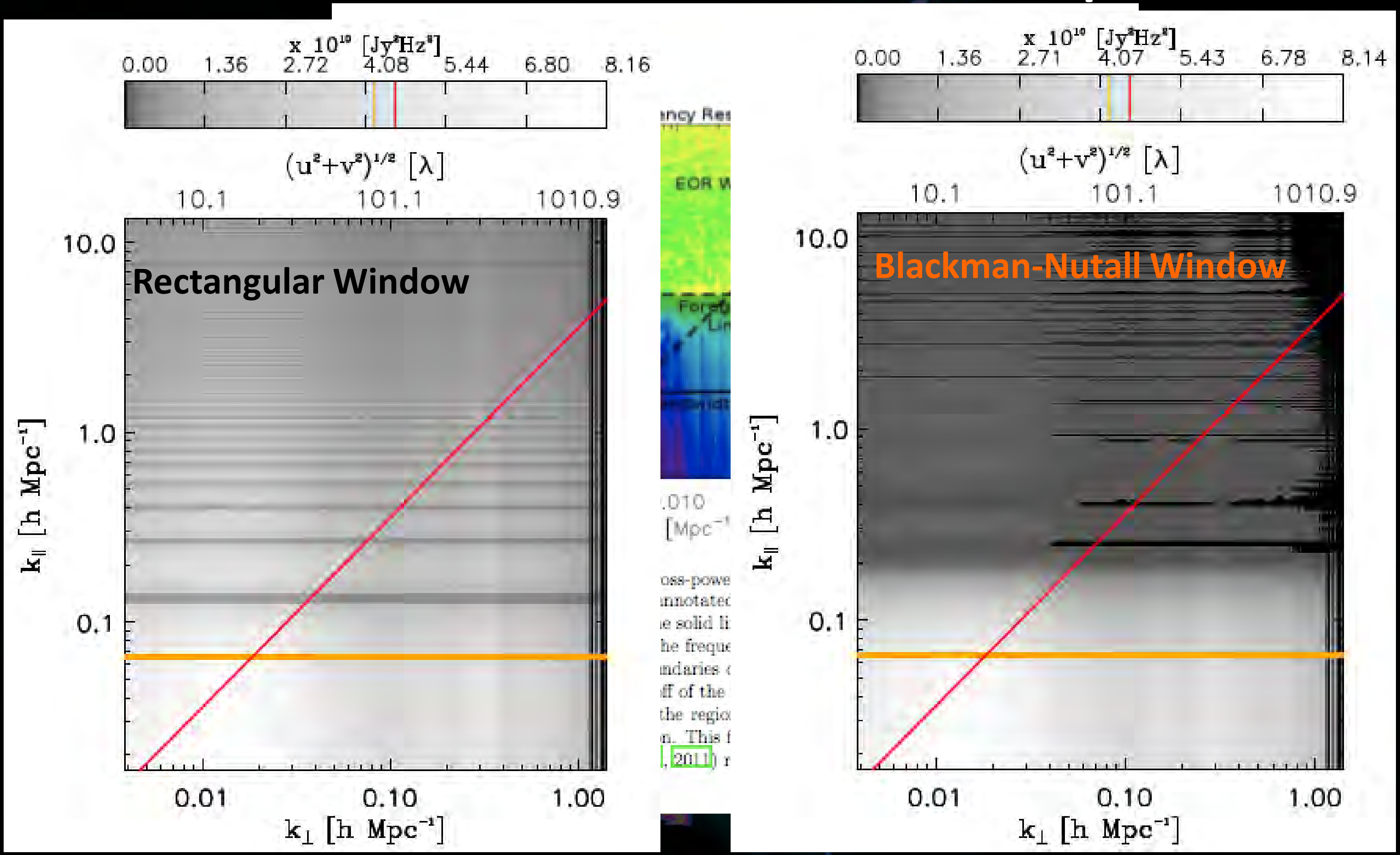

Delta function at $k_{||}$ = 0 spills over due to bandpass

Sidelobe Confusion

- Unsubtracted sources statistically represented by classical confusion is the source of sidelobes
- Sidelobes have frequency structure (results in mode-mixing)

Mode-mixing Principle

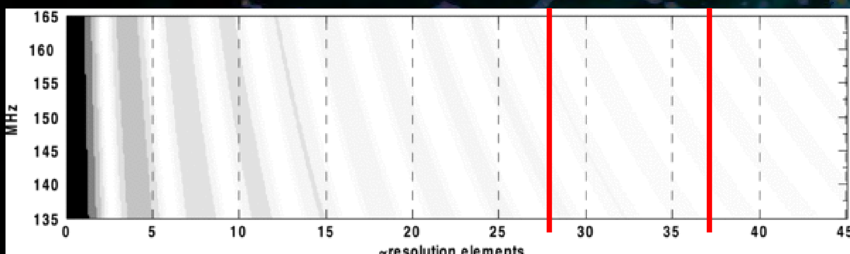

Bowman et al. (2009)

$$\eta_{cont} = u_{max}\, l / f$$

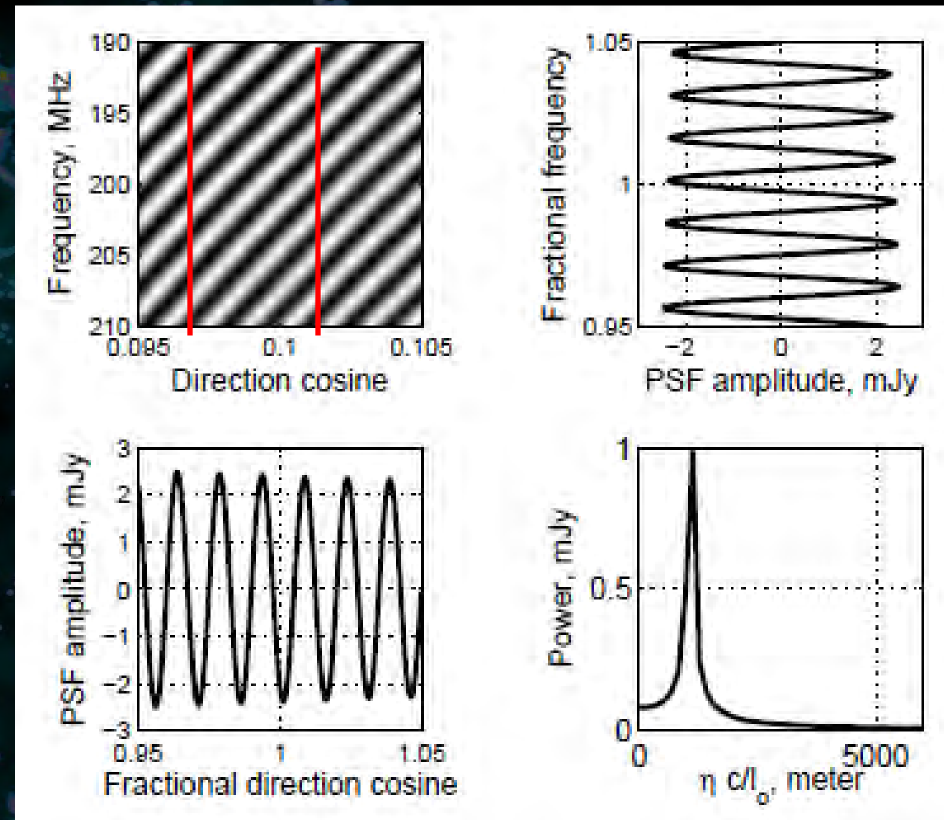

Vedantham et al. (2011)

Transverse structure of contamination translates to a line-of-sight structure due to mode-mixing l-f invariance

Sidelobe Confusion in *k*-space

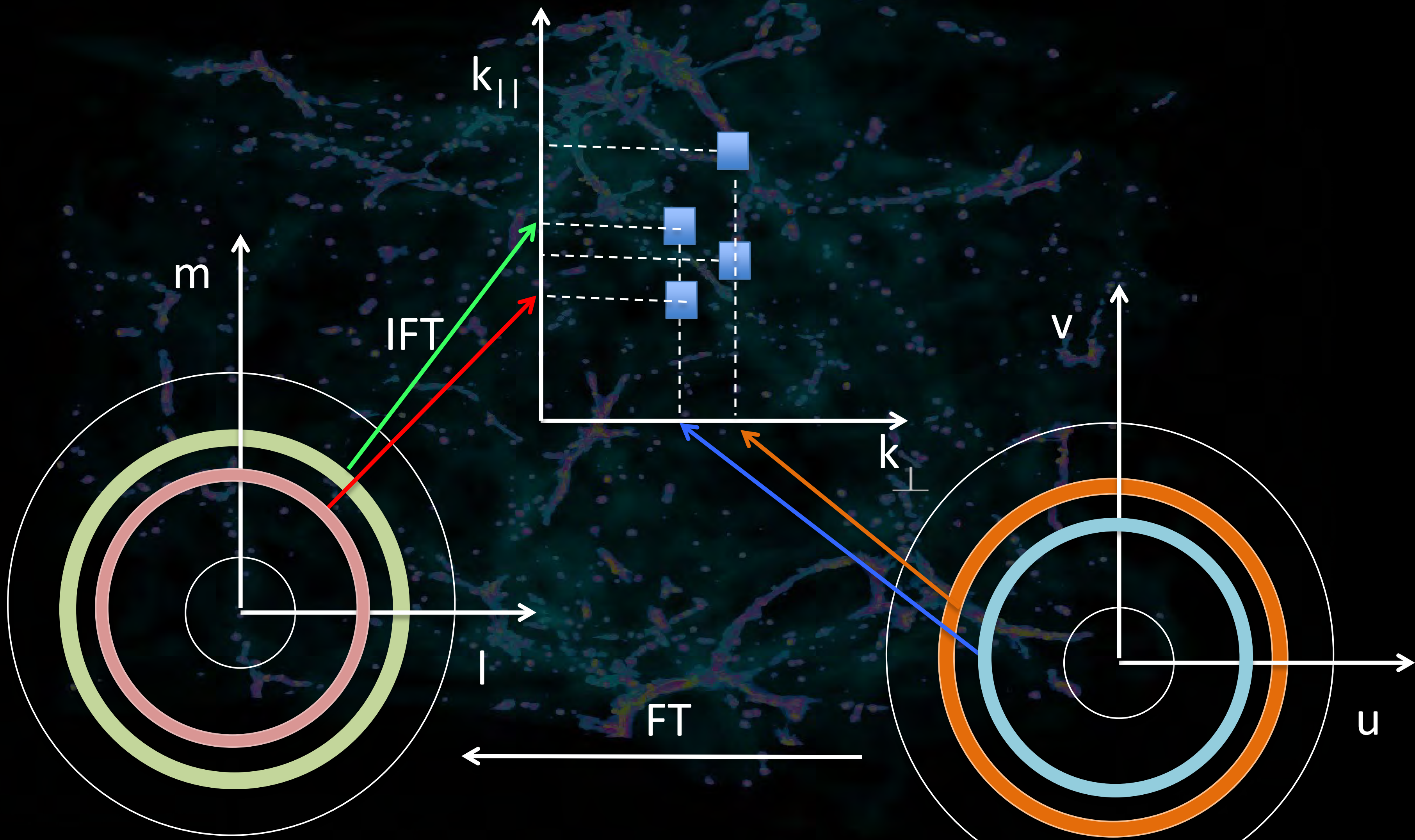

Sidelobe Confusion in *k*-space

Horizon
$(l^2+m^2=1)$

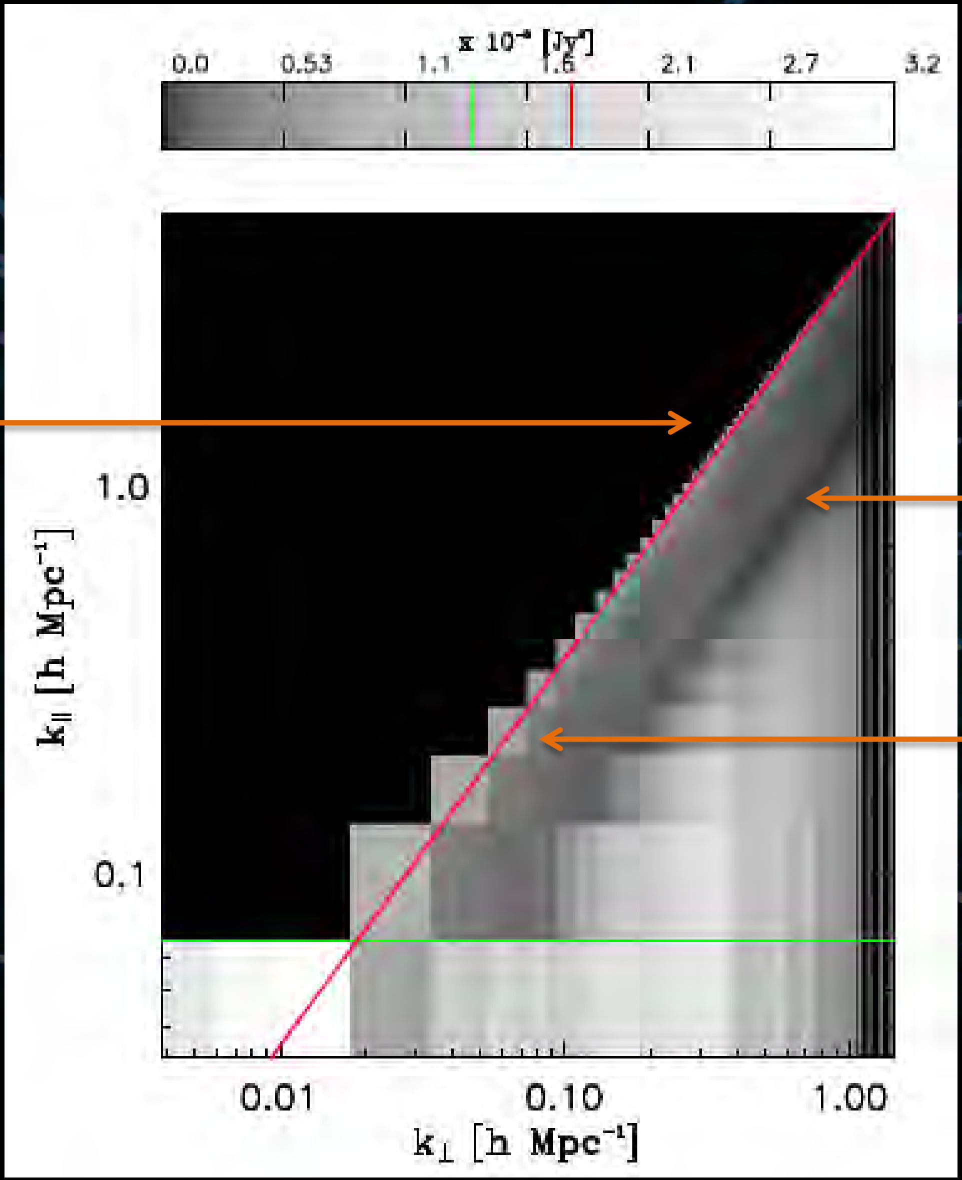

First null of
Primary Beam

Edge
Brightening

Sidelobe Confusion in *k*-space

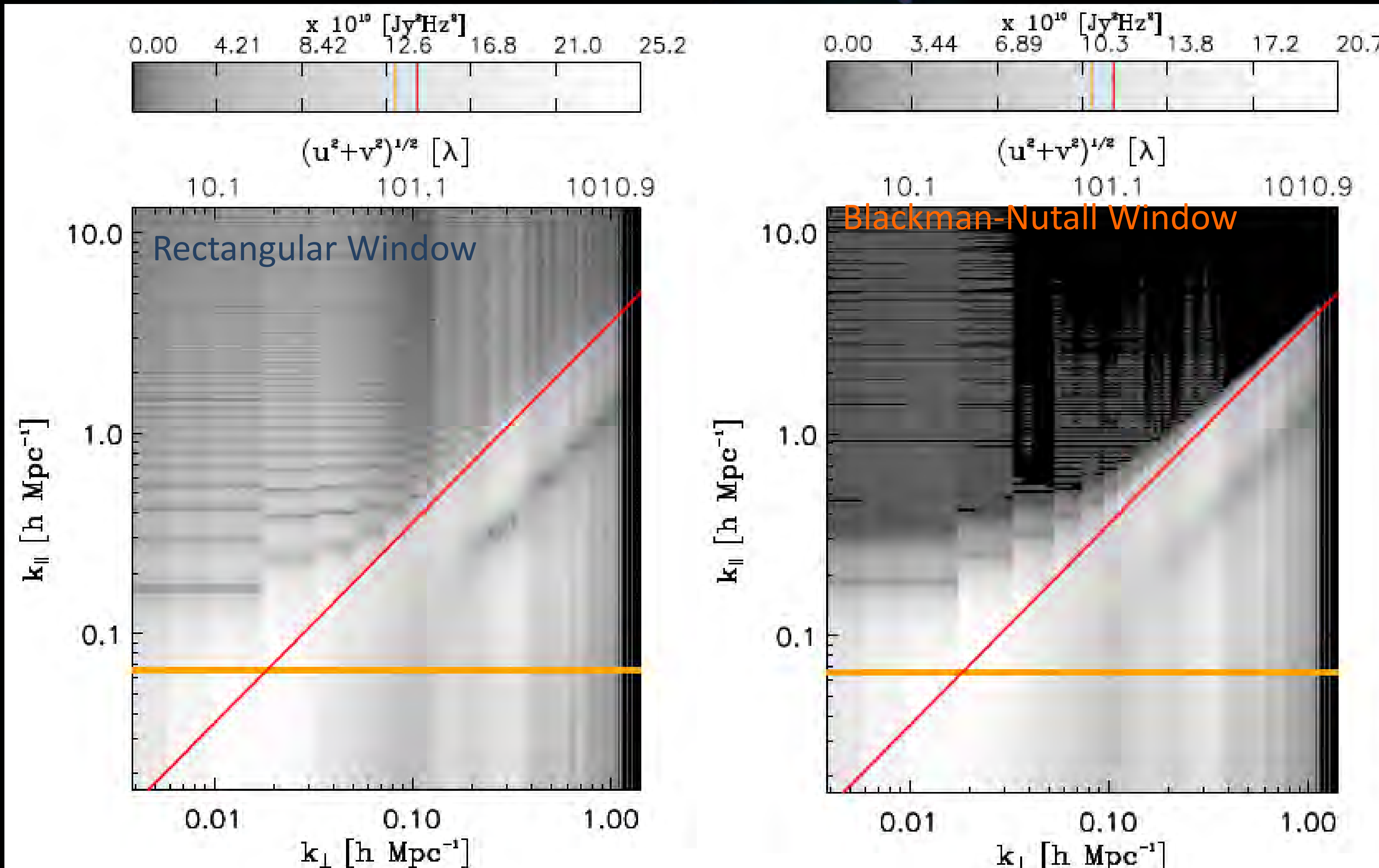

Observed Sensitivity in *k*-space

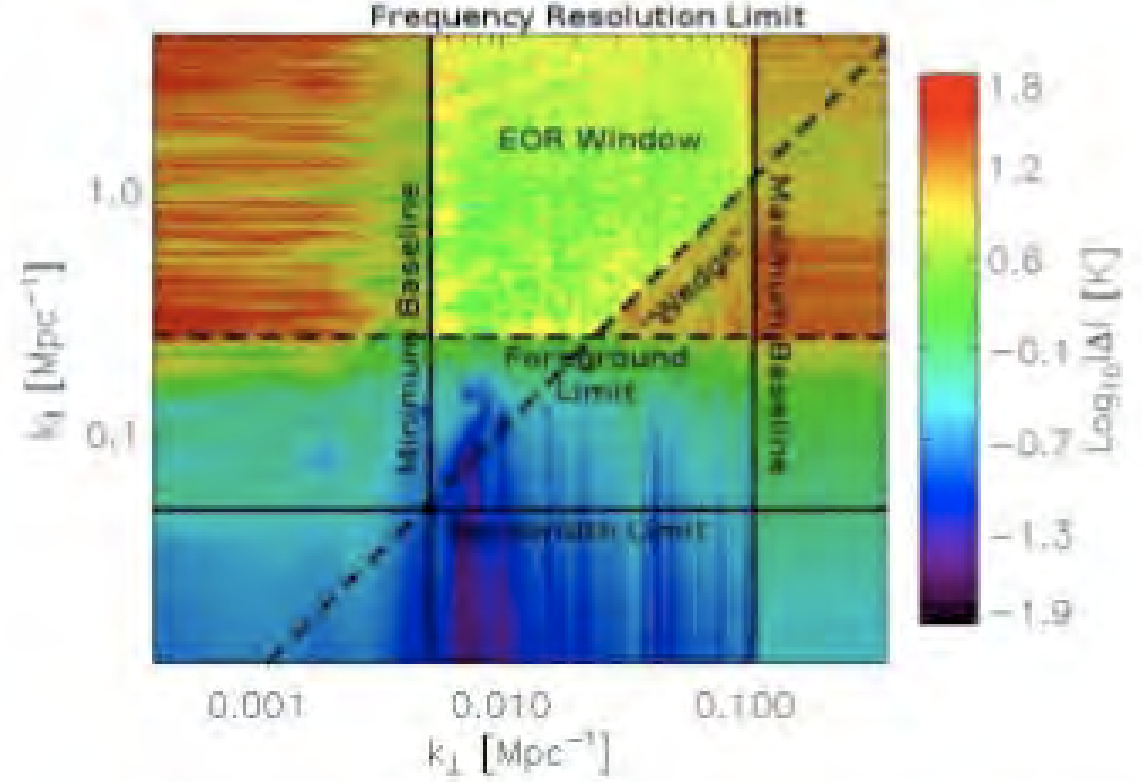

Figure 5-8: Beam-corrected FFT cross-power spectrum in the 142.645 MHz frequency band. Boundaries are drawn and annotated indicating the range accessible for EoR power spectrum measurements. The solid lines indicate fundamental limits governed by the geometry of the array and the frequency bandwidth and resolution. The dotted lines indicate approximate boundaries on various contaminants. The horizontal line indicates the approximate cutoff of the foreground principal component subtraction, while the "wedge" indicates the region bounded by a $k_{\perp} \propto k_{\parallel}$ line formed by point spread function contamination. This figure serves as an observed analog to the predictions from (Vedantham et al., 2011) reproduced in Figure 5-1

Thermal Noise

- $V_{rms}(u,v,f) = 2k_B T_{sys} / A_e (\Delta f\, \tau)^{1/2}$
- Thermal noise uniform along $k_{||}$
- Distribution along *k*-perp determined by Baseline distribution
- Integration time: 8 sec, 2 hours, 1000 hours

Thermal Noise in k-space

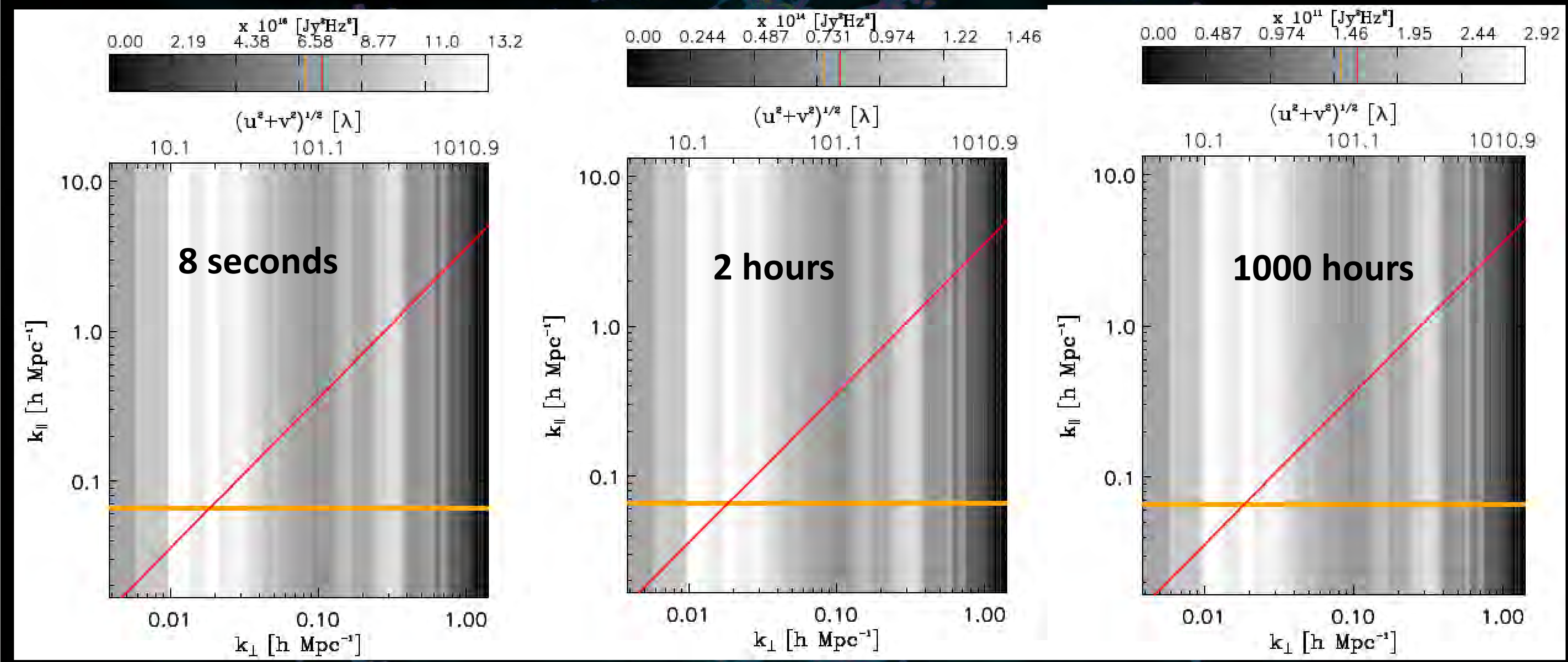

Combined Uncertainty

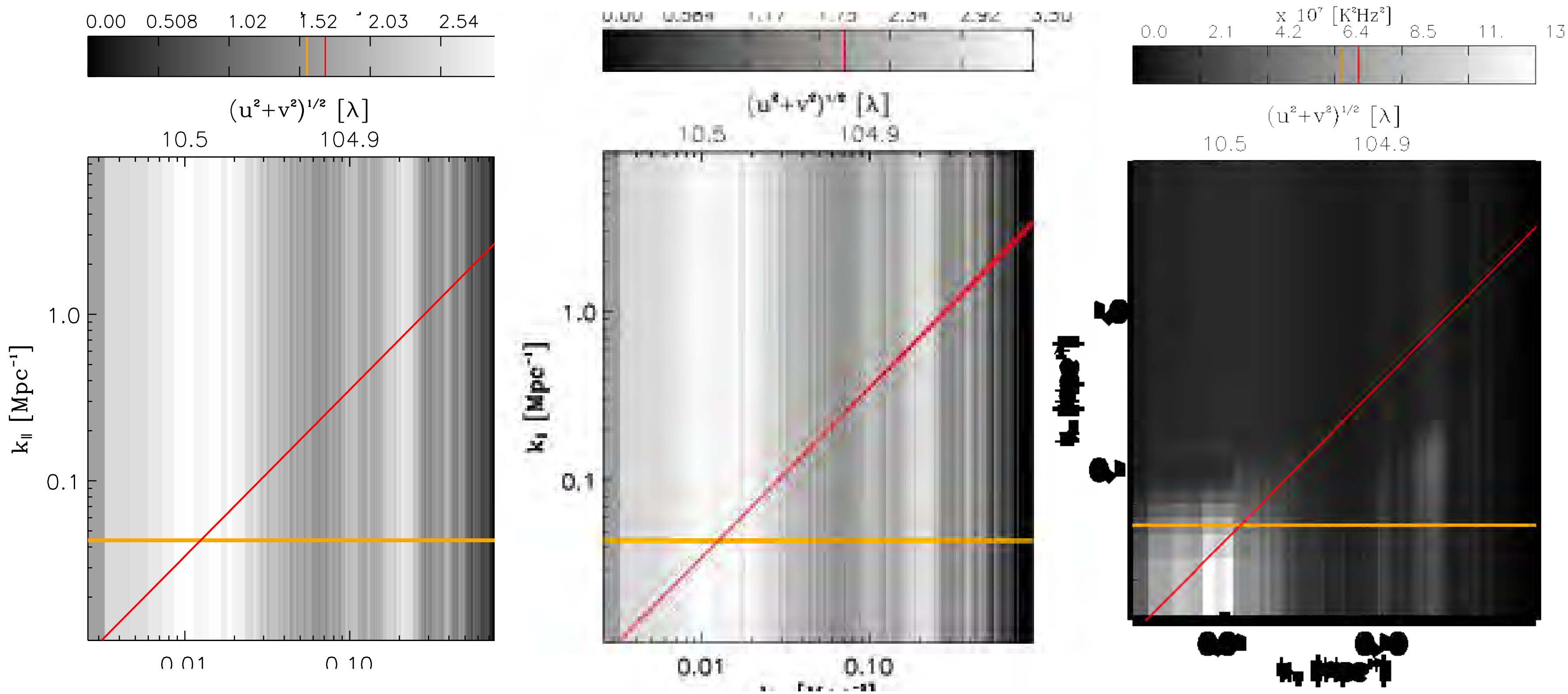

Model EoR Power Spectrum

- P(k) from Lidz et al.(2008) for z=7.32, ionization fraction=0.54
- Peculiar Velocity corrections applied

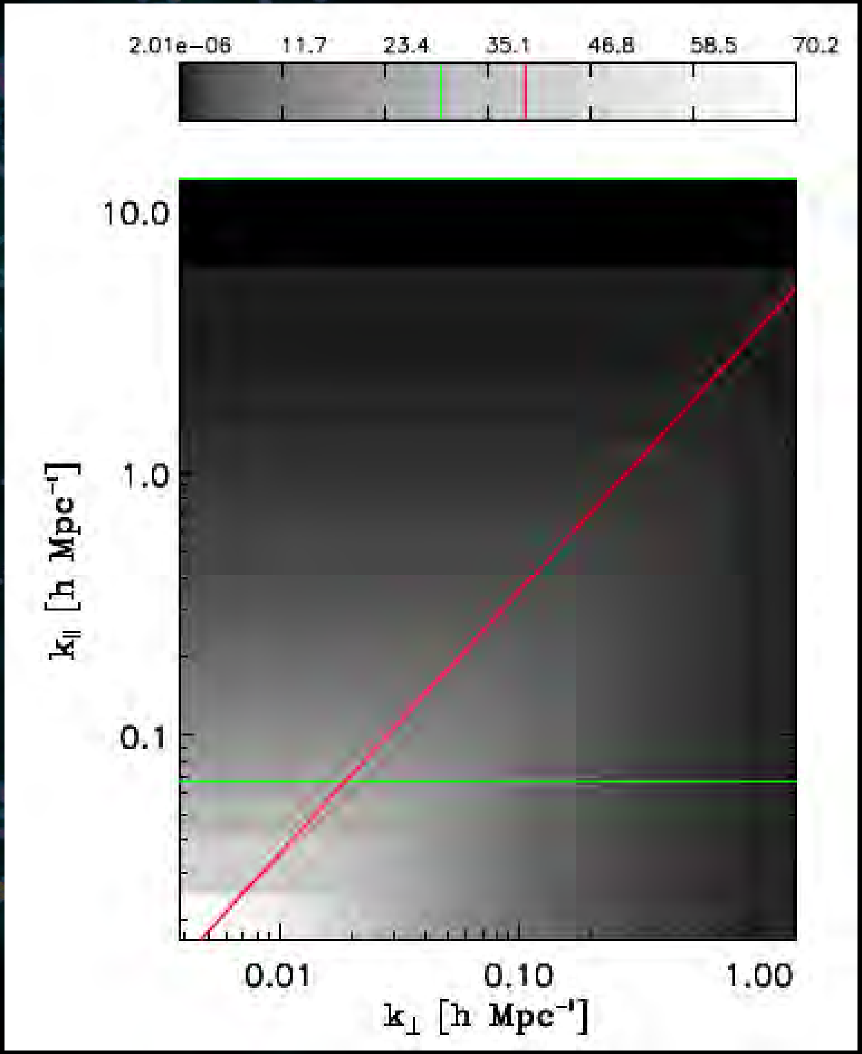

2D sensitivity (incl. sample variance)

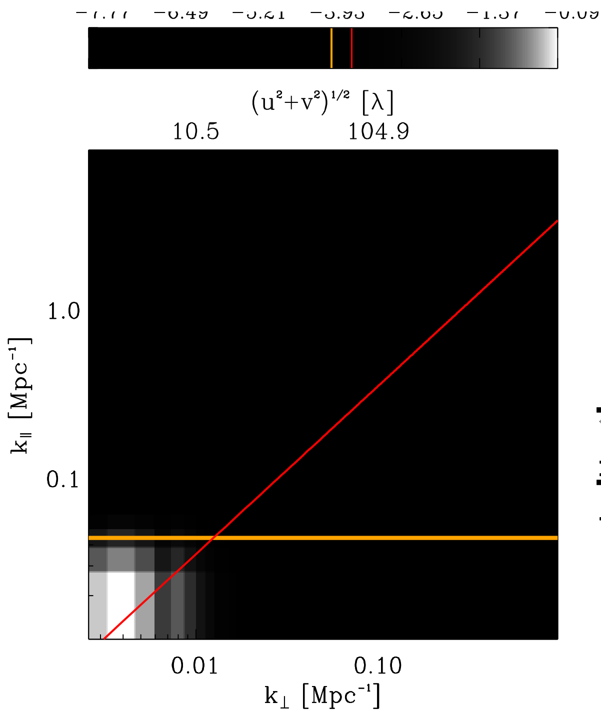

(a) *Blackman-Nutall* window, 8 sec-

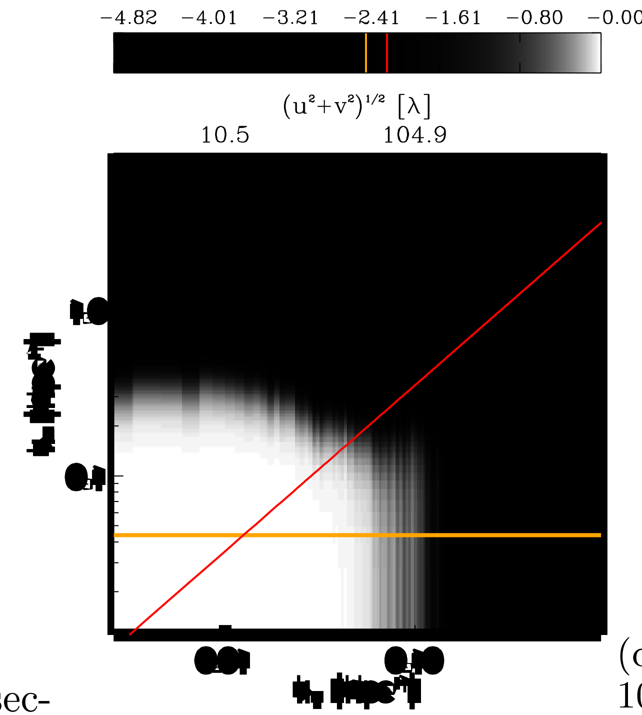

(b) *Blackman-Nutall* window, 2 hours

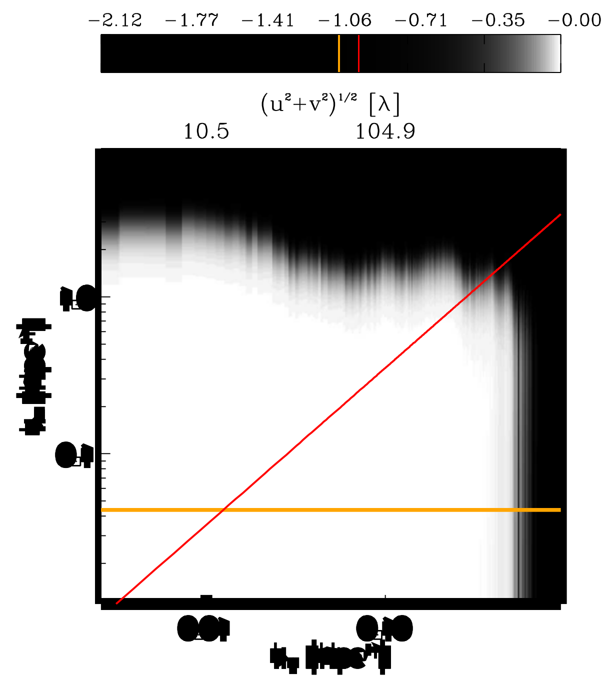

(c) *Blackman-Nutall* window, 1000 hours

Refined EoR windows

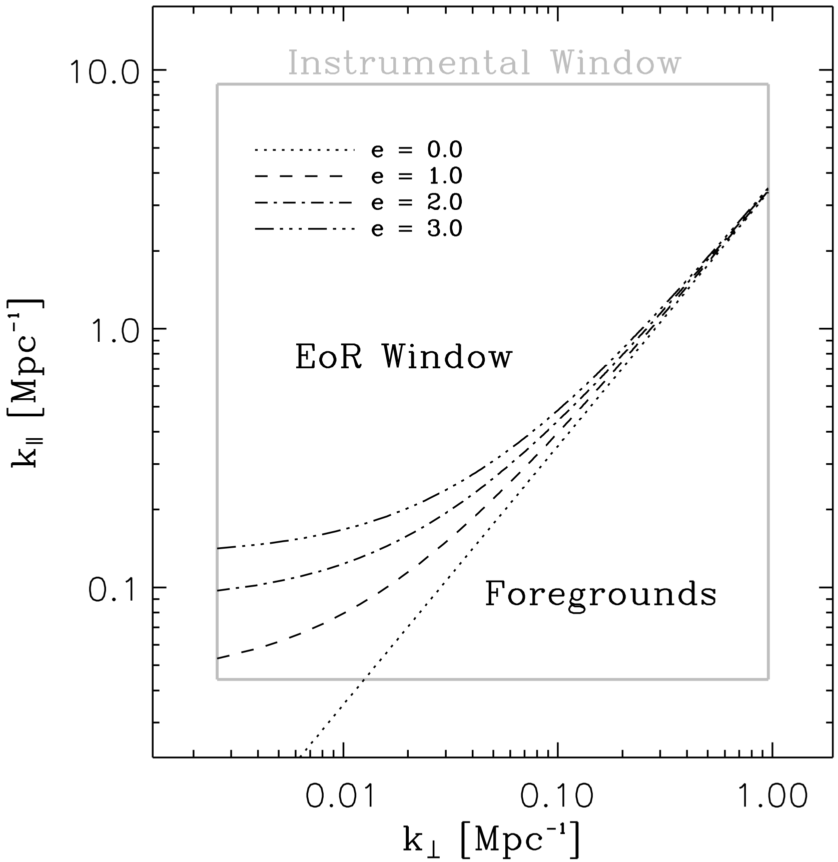

- Extra width due to convolution causing spillover
- Width ~ 1/B

Average in spherical shells in k-space

$$\overline{P(k)} = \frac{1}{N_k} \sum_{\substack{k_\perp, k_\parallel \\ k_\perp^2 + k_\parallel^2 = k^2}} P_{los}(k_\perp, k_\parallel), \quad \text{and,}$$

$$\frac{1}{\overline{\sigma^2(k)}} = \left[\sum_{\substack{k_\perp, k_\parallel \\ k_\perp^2 + k_\parallel^2 = k^2}} \frac{1}{[\sigma^2_{los}(k_\perp, k_\parallel)]^2} \right]^{1/2},$$

1D sensitivity

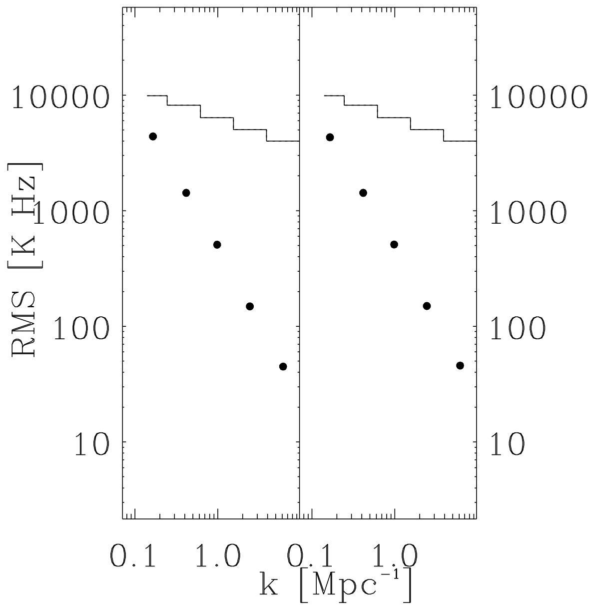

(a) 8 seconds

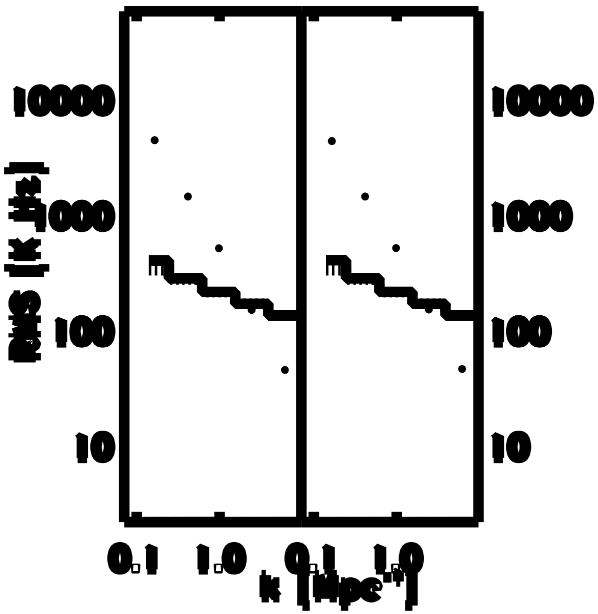

(b) 2 hours

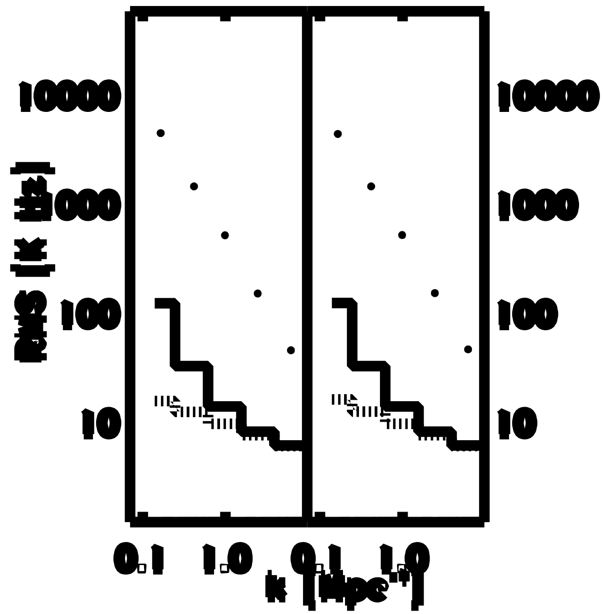

(c) 1000 hours

Conclusions

- Radio source statistics and 128T MWA layout
- Comprehensive estimate in k-space using
  1. Sidelobe confusion due to mode-mixing
  2. Classical Source Confusion
  3. Thermal Noise
  4. Sample Variance
- Array configuration has different effects on each
- Thermal Noise dominates on small scales
- Sample variance dominates on large scales
- Optimal choice of array and observing strategy (drfit-scan, tracking or hybrid)
- Compact arrays would give more sensitivity for EoR for future arrays?